

## Cancellation of Towing Ship Interference in Passive SONAR in a Shallow Ocean Environment

Remadevi M.<sup>#,\*</sup>, N. Sureshkumar<sup>#</sup>, R. Rajesh<sup>#</sup>, and T. Santhanakrishnan<sup>#</sup>

<sup>#</sup>*DRDO-Naval Physical and Oceanographic Laboratory, Kochi - 682021, India*

<sup>\*</sup>*Cochin University of Science and Technology, Kochi - 682 022, India*

<sup>\*</sup>*E-mail: remadevi@gmail.com*

### ABSTRACT

Towed array sonars are preferred for detecting stealthy underwater targets that emit faint acoustic signals in the ocean, especially in shallow waters. However, the towing ship being near to the array behaves as a loud target, introducing additional interfering signals to the array, severely affecting the detection and classification of potential targets. Canceling this underlying interference signal is a challenging task and is investigated in this paper for a shallow ocean operational scenario where the problem is more critical due to the multipath phenomenon. A method exploiting the eigenvector analysis of spatio-temporal covariance matrix based on space time adaptive processing is proposed for suppressing tow ship interference and thus improving target detection. The developed algorithm learns the interference patterns in the presence of target signals to mitigate the interference across azimuth and to remove the spectral leakage of own-ship. The algorithm is statistically analysed through a set of relevant metrics and is tested on simulated data that are equivalent to the data received by a towed linear array of acoustic sensors in a shallow ocean. The results indicate a reduction of 20-25dB in the tow ship interference power while the detection of long-range low SNR targets remain largely unaffected with minimal power-loss. In addition, it is demonstrated that the spectral leakage of tow ship, on multiple beams across the azimuth, due to multipath, is also alleviated leading to superior classification capabilities. The robustness of the proposed algorithm is validated by the open ocean experiment in the coastal shallow region of the Arabian Sea at Off-Kochi area of India, which produced results in close agreement with the simulations. A comparison of the simulation and experimental results with the existing PCI and ECA methods is also carried out, suggesting the proposed method is quite effective in suppressing the tow ship interference and is immensely beneficial for the detection and classification of long-range targets.

**Keywords:** Self noise cancellation; Towed sonar array processing; Tow ship interference cancellation; Target detection in Shallow Ocean; Spatio temporal processing

### NOMENCLATURE

SONAR	Sound navigation and ranging
LMS	Least mean square
CSDM	Cross-spectral density matrix
TOI	Targets of interest
STAP	Space time adaptive Processing
EVD/SVD	Eigen value/ singular value decomposition
ULA	Uniform linear array
STCM	Spatio temporal covariance matrix
SINR	Signal to interference plus noise ratio
SIC	Self interference cancellation
SNR	Signal to noise ratio
ORV	Ocean research vehicle
ADC	Analog to digital converter
PCI	Principal component inverse
ECA	Eigen component association
IBF	Inverse beamforming
∈	Belongs to
λ	Wavelength

### 1. INTRODUCTION

SONARs interrogate their surroundings with acoustic waves to detect and localise underwater targets and aid the naval forces to protect harbour assets while augmenting constant coastal surveillance. Active SONARs gather information about the target by acoustic transmission and monitoring their echoes, while passive SONARs listen to the noise emitted by the targets and detect them without revealing own presence. Generally, a long sensor array is towed behind the ship to reduce the strength of the tow ship radiation manifested on the array<sup>1</sup>. The low frequency signals emitted by the potential targets are better captured by towed arrays having a long aperture. They offer better resolution of targets and can be lowered to varying depths to take advantage of the ocean conditions. Towed arrays are widely used for long range submarine detection, oil exploration, seismic studies, ocean bottom profiling, and surveying<sup>2</sup>.

Though the sensor array is separated from the body of the towing ship, the strong noise emitted from the tow ship are picked up by the array through direct path and multipaths. This

interference adversely affects the detection and classification performances of the passive sonar. In a shallow ocean scenario, the multipath is dominant and the tow ship noise arrives at the sensor array through multiple angles depending on the ocean parameters. Detection, tracking and classification are the primary functions of a passive SONAR. The detection performance of the targets in the vicinity of tow ship bearing will be severely affected and tracks of the moving targets will be lost when it crosses the self-interference limited region. In a shallow ocean scenario, this problem is much more severe due to multipath propagation and bottom bounce reflections<sup>3-5</sup>. The acoustic field reflected from the sea bottom interferes with several beams in the azimuth, in addition to the direction of the towing ship. The classification performance is also severely degraded by the spectral leakage of the strong narrowband components radiated from the towing ship, into the spectra of TOI, which convolutes the feature vector extraction process. Therefore, this interference cancellation is inescapable to improve the performance of the passive sonar in shallow ocean conditions.

In the past decades, many methods have been developed to mitigate the effects of own platform noise. Traditionally, adaptive spatial filtering techniques and sectoral null steered beamforming methods are two popular approaches employed for the illustrated purpose<sup>6-9</sup>, which steers a null in the direction of the tow ship. However, this nulling reduces the interference only in a limited bearing interval. IBF based techniques are also employed<sup>10</sup>, where the interference is subtracted from received signals at the hydrophone in frequency domain, using iterative inverse beamforming. Li<sup>11</sup>, *et al.* proposed a combination of IBF and CLEAN algorithm, to improve the results of inverse beamforming, by removing sidelobes. IBF based schemes falters at severe multipath environment. Jia<sup>12</sup>, *et al.* presents a comparison of null steered beamformer and IBF.

Cheng<sup>13,14</sup>, *et al.* proposed a noise cancellation method for an autonomous underwater vehicle-towed thin line array through recursive adaptive filtering using variants of LMS algorithms. Sullivan<sup>15</sup>, *et al.* used a model-based approach employing an extended Kalman filter on this problem. These conventional adaptive cancellation approaches have relatively long convergence times and can have difficulty in suppressing nonstationary interferences from the tow ship. Lee<sup>16</sup>, *et al.* proposed a beamformer for detecting far-field sources in presence of near field interference. The steering vectors for a near field and far-field sources located in the same bearing are different, which is utilised for cancelling the near field interference. The method is easy to implement, but able to cancel near field interference only. Qiu<sup>17</sup>, *et al.* discusses a similar approach based on sparse Bayesian learning framework. Juan<sup>18</sup>, *et al.* has proposed a non-half wavelength towed array design for tow ship interference suppression.

Kirsteins<sup>19</sup>, *et al.* proposed principal component inverse (PCI) based method for interference suppression, where the rank of the interference subspace is estimated from the received data by analyzing the principal components of the spatial covariance matrix. However, the assumption of complete representation of the tow ship interference using principal components is not always valid. In order to identify

the complete interference subspace basis vectors, Harrison<sup>20</sup> proposed the Eigen Component Association (ECA) method for adaptive interference suppression. He used Eigen analysis on the Cross-Spectral Density Matrix (CSDM) and spatial filtering was carried out on each eigenvector to identify the basis vectors which span the interference subspace. The ECA method is able to rapidly adapt to the hierarchical swapping of the target and interference related eigenvectors due to relative signal power fluctuations and target dynamics. However, this method requires an approximate bearing of the TOI to compute the power ratio. Chen<sup>21</sup>, *et al.* combines the ECA approach and Kalman filter for joint interference suppression and target tracking. Zhang<sup>22</sup>, *et al.* summarises different approaches used for interference suppression in passive sonar and suggests space time-based schemes as prospective futuristic options. Most of the above-discussed methods aim at nulling the interference in a specified angular sector, while the beams and beam spectra corrupted by multipath reflections in multiple azimuth bearings are not discussed.

The problem statement can be summarised as the mitigation of tow ship interference arriving in the sensor array through multi-path, using higher dimensional space time adaptive processing-based subspace decomposition techniques, without affecting the detection performance of the long-range weak targets in a shallow ocean scenario. In prior literatures, most of the tow ship noise cancellation techniques are focused on:

- (i) Deep ocean scenario where the plane wave assumption is valid
- (ii) Subspaces are constructed using EVD / SVD on the estimated Spatial Covariance Matrix
- (iii) Efficient real time implementation of noise cancellation methods.

The performance of the existing noise cancellation methods discussed in the literature are bounded due to the smaller dimension of the array data vector. i.e., for an N element ULA, the dimension of the spatial covariance matrix is N by N and the subspace dimensions are less than N. Therefore, the complete characterisation of the tow ship acoustic field manifestation on the sensor array may not be possible with limited degrees of freedom, N. In a shallow ocean scenario, multiple normal modes contribute to the representation of the array field vector, where it is better to enhance the dimension of the problem for effective capturing of tow ship radiate noise manifested in the array.

In our proposed scheme, though the number of sensors is limited to N, the dimension of the problem is now increased to NK, where K is the number of time samples. In this work, EVD is performed on the space time covariance matrix (STCM) of dimension NK by NK. This enhanced degree of freedom leads to an efficient representation of the tow ship subspace. The shallow ocean experiments concluded that the proposed method is more efficient in mitigation of own platform noise in comparison with the existing methods. Thus, the novelty of the method can be considered as the extension of space time adaptive approach using higher dimensional space time covariance matrix, which is demonstrated to be very effective and appropriate for shallow ocean scenario. The shallow ocean

case assumes significance owing to the global shifting of naval warfare into littoral waters. Our major contributions are as follows:

- (i) Devised an algorithm for efficient mitigation of tow ship contributions in the array data vector using higher dimensional space time vector for complete characterisation of tow ship multipath radiations. Compared the results with the existing schemes.
- (ii) Validated the proposed scheme with sea trial data, thus establishing the efficacy of the method.
- (iii) Proven the proposed method for multipath ridden shallow ocean scenario

## 2. SYSTEM GEOMETRY AND ARRAY MODEL

In a shallow water environment, the acoustic propagation is guided by the sea bottom and surface as in a waveguide. We modelled the ocean as a horizontally stratified water medium of constant depth  $h$  overlying a bottom<sup>23</sup>. This model assumes that the ocean is range-independent, i.e., variation of its acoustic properties in the horizontal direction is negligible in the range of our interest.

Figure 1 shows the source-receiver geometry. Consider a narrowband point source having a center frequency  $\omega_0/2\pi$  and  $p'_j(t)$  as the slowly varying envelope of the signal, set in a shallow ocean environment. The source is located at  $(r_j, \theta_j, z_j)$  where  $r_j$  is the range of the source,  $\theta_j$  is the azimuthal direction with respect to the end-fire of the array and  $z_j$  is the source depth. We apply normal mode theory to characterise the propagation of the acoustic signal in a shallow ocean. During the propagation, several modes are generated in the vertical direction. It is fair to assume that all the energy is trapped in the stationary waves of the waveguide, and the resultant acoustic field can be obtained by combining the significant modes<sup>24</sup>.

The acoustic pressure field reaching the array elements is the sum of normal modes and an integral of the continuous modal spectrum<sup>24</sup>. It may be noted that this intensity is independent of the azimuth  $\theta_j$  due to the assumption of horizontally stratified ocean. Far-field spatial distribution of the resulting pressure signal originating from a source at  $(r_j, \theta_j, z_j)$ , ignoring the negligible contribution due to continuous modal spectrum, is well approximated by a sum of  $M$  discrete normal modes<sup>25</sup> and is given by

$$p(r_j, z_j, t) = \left( \sum_{m=1}^M q_{mj} \right) p'_j(t) e^{-j\omega_0 t} \quad (1)$$

where,

$$q_{mj} = \left( \frac{2\pi}{k_m r_j} \right) \Psi_m(z_j) \Psi_m(z) e^{(-\alpha_m r_j - (k_m r_j - \pi/4))} \quad (2)$$

where  $z$  is the array depth and  $m$  is the mode number.  $\Psi_m(z)$  is the eigen function while  $k_m$  is the eigenvalue obtained as the solution of the Sturm-Liouville characteristic differential equation,

$$\frac{d^2 \Psi_m(z)}{dz^2} + [k^2(z) - k_m^2] \Psi_m(z) = 0 \quad (3)$$

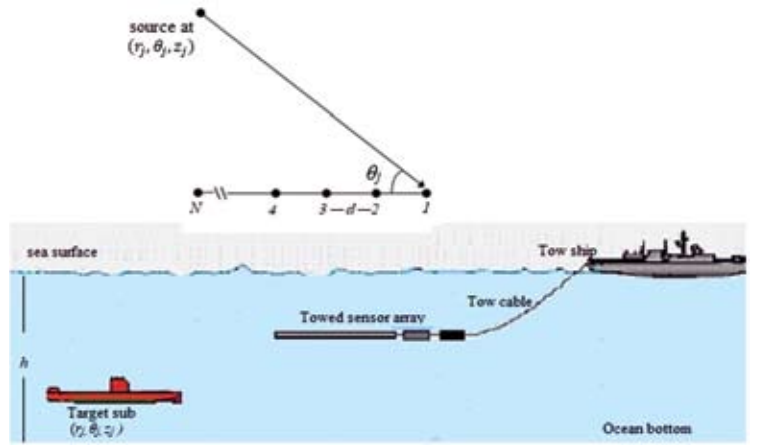


Figure 1. ULA sensor geometry and source locations in ocean medium.

where  $k = \omega/c$  is the wavenumber,  $c$  is the sound speed in the water layer at depth  $z$ , and  $\omega$  is the angular frequency. Consider the case of a linear horizontal array having  $N$  sensors uniformly placed with inter sensor spacing,  $d$ . Let  $J$  narrowband sources of center frequency,  $f_0$  be located at depths  $z_j$  ranges  $r_j$  ( $j=1, \dots, J$ ) and at an azimuthal angle  $\theta_j$ , relative to the front end fire of the array. The signal received at the first sensor of the array is given by (1). The output corresponding to  $N$  hydrophones of the array may be expressed as the vector

$$y(t) = [y_1(t) \dots y_N(t)]^T = P(X) \tilde{p}(t) + w(t) \quad (4)$$

where  $\tilde{p}(t) = [p'_1(t) \dots p'_J(t)]$  is the source signal vector,  $p'_j(t)$  being the slowly varying complex amplitude of the signal from the  $j^{\text{th}}$  source, modelled as jointly stationary and uncorrelated circular complex Gaussian random process.  $w(t) = [w_1(t) \dots w_N(t)]$  captures the noise experienced at the array. We model them as the independent and identically distributed circular complex Gaussian random variables with variance  $\sigma^2$ .

$$P(X) = [p(x_1) \dots p(x_J)] \in C^{(N \times J)}, \quad x_j = [\theta_j, r_j, z_j]^T \quad (5)$$

$P(X)$  is an  $N \times J$  matrix whose columns

$$p(x_j) = [p_{j1} \dots p_{jN}]^T \in C^{(N \times 1)} \quad (6)$$

corresponds to the signal levels received by the array. The vectors  $p(x_j)$  can be written in terms of mode amplitude vectors and steering vectors as

$$p(x_j) = B(\theta_j) q(r_j z_j), \quad j=1, \dots, J \quad (7)$$

where,

$$q(r_j, z_j) = [q_{1j} \dots q_{Mj}]^T \quad (8)$$

are the mode amplitude vectors whose elements  $q_{mj}$  are defined by (2), and

$$B(\theta) = [b(k_1 \cos \theta) \dots b(k_M \cos \theta)] \in C^{(N \times M)} \quad (9)$$

where the columns represent the array steering vectors given as

$$b(k_m \cos \theta) = [1 \ e^{(ik_m d \cos \theta)} \dots e^{i((N-1)k_m d \cos \theta)}]^T, \quad m=1, 2, \dots, M \quad (10)$$

The theory can be extended to the broadband case, as the broadband signal is composed of uniformly spaced narrow band components over the band of interest.

### 3. SPACE TIME ADAPTIVE PROCESSING

STAP, which is a filtering action in both space and time, a multi-dimensional signal processing technique, provides significant improvements in various fields such as surveillance radars, wireless radio communications, and underwater sonar systems<sup>26,27</sup>.

The work by Brennan<sup>28</sup>, *et al.* introduced an adaptive system that senses the angular-doppler distribution of the external noise field and adjusts a set of parameters to maximise signal-to-interference ratio and optimum detection performance. Target and clutter in space and time can be simultaneously differentiated.

Let the data received at the  $N$  elements of a ULA are sampled and the sample size is  $K$ . We get an array data matrix of size  $K \times N$ . This sampling operation is repeated at  $L$  successive time intervals. Thus, we get a  $K \times N \times L$  array, during each coherent processing interval. This can be viewed as a data cube with slices of size  $K \times N$  stacked linearly. Then the associated space-time data can be taken as  $Y$  with size  $K \times N$ , each column representing the data received at each sensor.

The space-time processing can be described as a linear weighting  $W$  of the received data  $Y$ , with a constraint to remove the noise present in the received array data vector. It has been proved that the optimum weight is

$$W = uR^{-1}s \quad (11)$$

where  $u$  is a constant,  $s$  is the target steering vector and  $R$  is the noise covariance matrix. In practical cases,  $R$  is to be estimated from the array data samples. The maximum likelihood estimation of  $R$  is done by averaging  $L$  blocks of the array data snapshots.

In the fully adaptive STAP method, the covariance matrix is estimated using large sample sets of interference and noise. The large matrix dimensions hugely increase the computational complexity of this approach. It is imperative to develop algorithms that make use of reduced dimensions. In this paper, we employ a reduced rank space-time processing algorithm, customised for passive sonar context.

### 4. PROPOSED METHOD

We exploit the space time covariance matrix subspace projection based methods<sup>27,29,30</sup> and Eigen analysis based adaptive methods<sup>31,32</sup> for tow ship interference cancellation. Consider the data model of an  $N$  element ULA described in Section 2. The interference generated from the tow ship can be considered as a strong signal in the end-fire direction of the array axis and effectively  $J - 1$  acoustic sources are only available for modelling the TOIs.

Since the tow ship is very close to the sensor array, compared to any possible targets, it can be safely assumed that the space-time array data vector contains dominantly the interference generated by the tow ship. From the array data matrix  $Y$ ,  $K$  time samples corresponding to each sensor of the array, are stacked to form a  $KN \times L$ , concatenated vector  $\mathbf{x}$ .

$$\mathbf{x} = [y_1^T \ y_2^T \ \dots \ y_K^T]^T \in C^{(KN \times L)}, \quad y_k \in C^{(N \times L)}, \quad k = 1, 2, \dots, K \quad (12)$$

The space time covariance matrix  $R$  is formed by averaging over  $L$  subsequent data blocks of the concatenated

array data vector  $\mathbf{x}$ .

$$R = E(x_i x_i^H) = \frac{1}{L} \sum_{i=1}^L x_i x_i^H \in C^{KN \times KN} \quad (13)$$

The Eigen decomposition of the STCM is carried out to compute the eigenvectors corresponding to the dominant eigenvalues. The interference signal can be effectively represented as a linear combination of the principal spatio-temporal eigenvectors of STCM. In practice, setting the threshold on the rank of the interference subspace is a very critical and involved process. We explored a method based on Gerschgorin Disk estimation<sup>33,34</sup> to threshold the dominant vectors. We also attempted another method based on adaptive identification of dominant eigenvectors<sup>32</sup>. This second method turned out to be more robust for practical scenarios. We have customised it for shallow ocean multi-modal scenarios by using multiple steering vectors corresponding to the dominant propagation modes to steer the beam in the given direction. Define a matrix  $V$  which is constructed using  $g$  dominant eigenvectors of  $R$ , assuming that these eigenvectors correspond to that of self-noise. Then the null space of  $V$  is given by

$$Z = I - VV^H \in C^{(KN \times KN)} \quad (14)$$

where  $I$  is the identity matrix, clearly  $Z$  is the space orthogonal to the self-interference. In fact,  $Z$  is the projection matrix and this phase of the process can be considered as a learning phase of the algorithm. Now consider the real scenario where the received signal contains several targets as well as self-interference. To remove the effect of self-interference, the sensor array signals  $x$  are projected onto  $Z$  as

$$z = Zx \in C^{(KN \times 1)} \quad (15)$$

This can be considered as a pre-processing technique. A response function is applied to this transformed data  $z$ . It is important to identify an appropriate response function to evaluate the proposed pre-processing technique. Conventional frequency domain beamforming in conjunction with energy detection is selected as the response function because it performs uniformly in all azimuthal directions, unlike adaptive methods where the response is non-uniform and introduces nulls<sup>35</sup>. The response function is applied on the projected data  $z$ , to estimate the bearing of TOI. Algorithm 1 summarises the proposed towing ship interference cancellation technique. Figure 2 illustrates the flow diagram representing the steps leading to SIC.

---

#### Algorithm 1: The Steps Leading to Towing Ship Interference Cancellation

---

- Input: Array data matrix  $Y \in C^{(T_f \times N)}$ ,  $f_s$  - sampling frequency &  $T$  - observation time
- 1: Read  $K$  snapshots from  $Y$  to form the concatenated vector  $\mathbf{x} \in C^{(KN \times 1)}$
  - 2: Estimate STCM by averaging  $T/K$  blocks of data,
 
$$R = \frac{K}{T} \sum_{i=1}^{T/K} x_i x_i^H, R \in C^{(KN \times KN)}$$
  - 3: Compute eigenvalue decomposition on  $R$
  - 4: Construct self-interference subspace  $V$  using  $g$  dominant Eigenvectors of  $R$ ,  $V \in C^{(KN \times g)}$

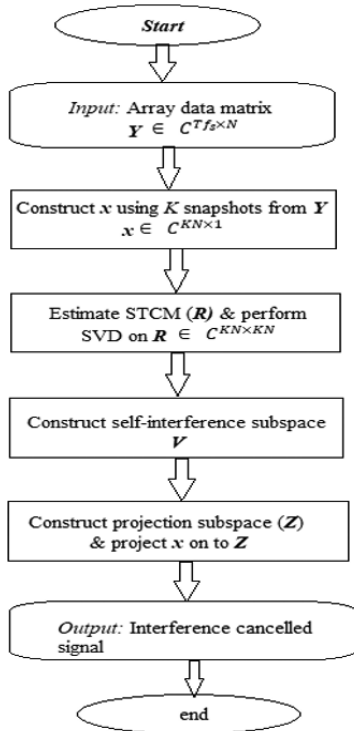


**Figure 2. Flow diagram of steps leading to towing ship interference cancellation.**

- 5: Compute projection space  $Z = I - VV^H$ ,  $Z \in C^{(KN \times KN)}$
- 6: Project the concatenated vector  $x$  on to the projection matrix  $Z$  to obtain the tow ship interference cancelled signal

In this work, the tow ship interference signal is completely captured in a subspace using a large number of Eigen basis vectors derived from the high dimensional space time covariance matrix. The STCM enhances the degrees of freedom and hence is capable of effectively representing the interference signal. Though the computational complexity of this proposed method is high compared to PCI<sup>19</sup> and ECA<sup>20</sup>, the tow ship interference suppression performance is superior. It is noteworthy that, the experiments conducted in a horizontally stratified ocean with a constant towing speed, it is observed that, the spanning basis vectors of the tow ship signal subspace does not change drastically with respect to time and hence STCM decomposition can be performed in the order of minutes. In addition, in this method, STCM is computed for the wideband signal (Narrowband STCM is not effective) which further reduces the required FLOPS for real time implementation of the proposed technique.

## 5. SIMULATION RESULTS AND ANALYSIS

### 5.1 Simulation Environment and Training Parameters

We have evaluated the proposed method through extensive Monte Carlo simulations. We simulated the tow ship interference

along with TOI signals embedded in ambient noise as received by a horizontal ULA of 32 sensors spaced at 0.1875 m, which is half wavelength corresponding to 4 kHz. The height of the water column is assumed to be 100 m and receiver depth 35 m. The attenuation is assumed as 0.25 dB/km, in our frequency range of interest in Indian waters. During simulation, the mode values and Eigen functions for the shallow ocean environment were computed using the well-accepted KRAKEN program based on normal mode theory<sup>36</sup>. Provided the sound speed profile and ocean bottom parameters, KRAKEN computes the mode-functions and the mode values for the range-invariant ocean, using which the received acoustic pressure at the array is arrived at Table 1 illustrates the simulation parameters.

### 5.2 Simulation Results

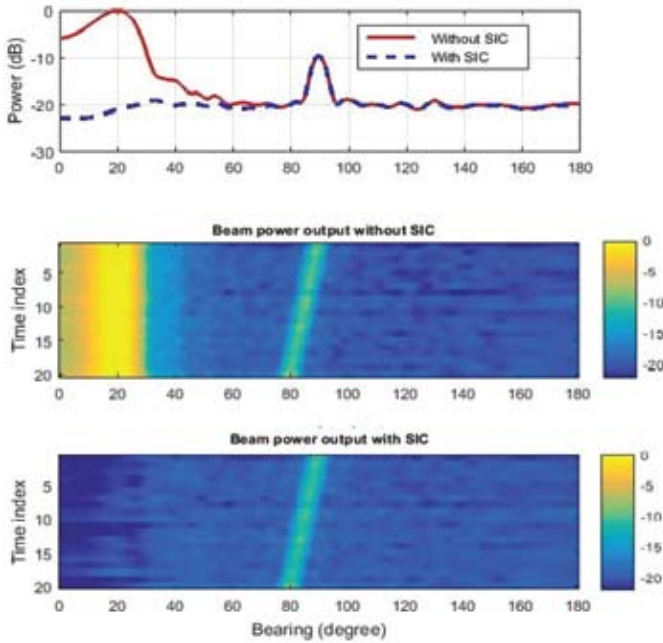
The acoustic signature generated by the tow ship is simulated at an azimuth direction of 20° with respect to the ULA axis in a frequency band of 2 kHz to 4 kHz. This signal acts as the interference. The tow ship is positioned close to the ocean surface with a lateral range separation of 350 m from the first sensor of the array. The TOI is simulated at 40 m depth, moving with azimuth bearing rate 0.5 deg/sec, having the similar acoustic band of tow ship interference. The range of the TOI is adjusted so that the TOI signal power is approximately 6 dB less than the tow ship interference power received at the sensor output. Along with this, shallow ocean ambient noise is generated<sup>37</sup> and is added to the array data vector. The ambient noise power level is adjusted to maintain roughly -10 dB SINR at the sensor output. In this simulation, 32 consecutive array data vector snapshots (time samples of 32 sensors) are used to form a concatenated vector of length 1024 and is processed further to estimate the STCM and the projection matrix. In all the cases, the STCM was computed by averaging 300 concatenated spatio-temporal array data vectors. Since the primary focus is on evaluating the performance of the pre-processing technique to remove the tow ship interference, a conventional frequency domain beamformer followed by an energy detector is used as a response function. The bearing estimates are presented after averaging through 200 Monte-Carlo simulations.

Figure 3 shows the beam output power with and without the application of the SIC technique, in both amplitude graph and waterfall format. In the amplitude graph generated before SIC, two peaks are observed, one at 20° and the second one at 90°. The former one is due to the self-noise of the platform and the latter corresponds to the TOI. The amplitude graph also shows the result of the proposed SIC scheme. It can be observed that the interference due to tow ship noise at 20° azimuths is reduced considerably while the target present at 90° is unaffected.

The waterfall diagram depicts the scenario where a TOI is an opening target starting from 80° and moving away from the tow-ship to 90°. It is the beam power output providing the history of tow-ship and TOI over time, indicating the tow-ship

**Table 1. Simulation parameters**

No of sensors	Inter element spacing (m)	Rx depth (m)	TOI depth (m)	Freq band (kHz)	Water column depth (m)	No. of Monte-Carlo runs
32	0.1875	35	40	2 - 4	100	200

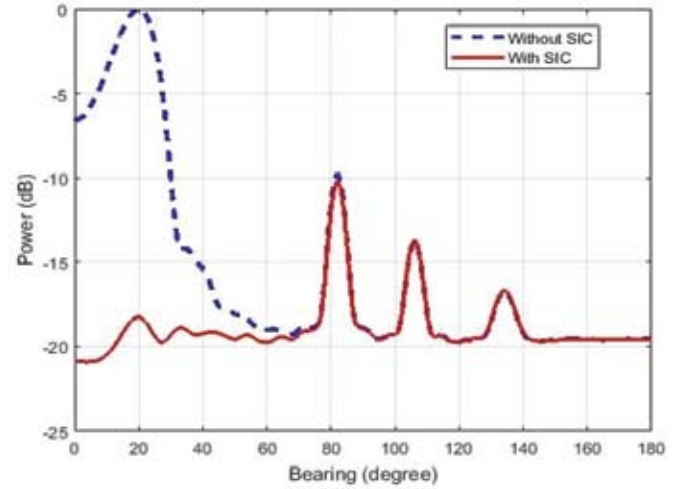


**Figure 3.** Beam power output with and without SIC algorithm. Current position of TOI bearing at  $90^\circ$  and own ship interference at  $20^\circ$  in the amplitude graph. Waterfall plot also shows the beam power output without and with SIC algorithm indicating the history of target positions.

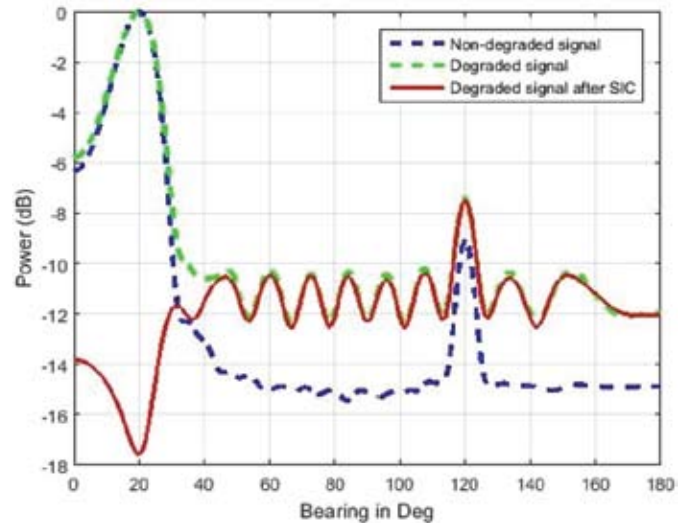
interference cancellation after the SIC, proving the efficacy of the proposed algorithm. The amplitude graph corresponds to the latest position of the target given in the waterfall plot.

Figure 4 demonstrates the performance of the proposed technique in the presence of multiple targets positioned at different azimuth bearings and ranges. Three acoustic sources are positioned at depth 40 m with bearing angles of  $82^\circ$ ,  $106^\circ$ , and  $134^\circ$  and ranges are adjusted such that the acoustic sources produce SINRs -10 dB, -14 dB, and -18 dB respectively. The response function (dotted blue line) produces 4 peaks whose positions match well with the interference and source azimuth bearings. In the response function without SIC, the peak at  $20^\circ$  corresponds to the tow ship interference. The solid red line depicts the response function with the SIC algorithm which clearly shows the effective removal of interference components without affecting the detection and localisation performance of multiple sources. The proposed algorithm effectively identifies the strong spatio-temporal coherence components using STCM and projecting it out from the received array data vector. It is also observed that the detection and localisation performance of weak SNR targets are unaffected with the application of SIC pre-processing technique.

To test the robustness of the scheme, perturbations are introduced in the sensor array data vector. In the frequency domain, this is achieved by component-wise multiplication of an array data matrix with a perturbation matrix, which is generated for a specified sensor and associated signal conditioning perturbation level. The perturbation matrix consists of complex elements which effectively captures the imperfections in the sensor and data acquisition hardware. Figure 5 is generated with a perturbation matrix which



**Figure 4.** Beam power output of three target cases with and without SIC applied. Targets are at  $82^\circ$  (SINR -10 dB),  $106^\circ$  (SINR -14 dB),  $134^\circ$  (SINR -18 dB) and own ship interference at  $20^\circ$ .



**Figure 5.** Beam power output for degraded channel case and non-degraded signal case with and without SIC applied. Target is at  $120^\circ$  and tow ship interference is at  $20^\circ$ .

introduces random amplitude and phase distortion for all the sensor outputs by 10% of its true value. Also, we have injected a narrowband component of 3 kHz in 10% of randomly selected sensors. The tow-ship noise is at  $20^\circ$  and the target is at  $120^\circ$ . It may be observed from the figure that channel degradation does not reduce the effectiveness of the algorithm.

From the simulation results, it is clear that source localisation with the proposed algorithm mitigates the effect of self-interference effectively. Moreover, the lower SNR target detection is not perturbed by the algorithm, which is a crucial result for towed array applications. It is to be mentioned that the algorithm learns the self-noise pattern in the presence of TOIs, which is the realistic scenario.

### 5.3 Power Loss Evaluation

The performance of the proposed scheme is characterised by measuring the power loss that occurred in the TOI signal



under various operating conditions. This metric is computed as the difference in the response function output at the TOI bearing with and without SIC for a specified interference suppression.

Figure 6 shows the power loss of the TOI signal using the proposed SIC method under various operating conditions. Fig. 6(a) shows the power loss associated with the TOI versus SINR for different source bearings (60°, 90°, 120°) while positioning the tow ship at 20°. The SINR of TOIs is varied from -6 dB to -24 dB to study the power loss performance of SIC with respect to SINR. It is observed that the power loss associated with higher SINR targets are high and decreases with a decrease in SINR, with the power loss being negligible for distant weak targets. This is well justified due to the fact that the Eigen components corresponding to the strong acoustic sources are likely to fall in the set of basis vectors that span the interference Eigen space. However, the weak TOI completely occupies the Eigen subspace which is orthogonal to the dominant vectors spanning the interference space, as expected. Since the towed array sonar design is aimed to detect long-range weak SNR targets, the power loss results encourage the use of the proposed pre-processing technique for suppressing the clutter in the response function.

The power loss with the angular separation between the tow ship and TOI for various SINR conditions (0 dB, -5 dB, -10 dB) is illustrated in Fig. 6(b). Here, the interference is fixed at an angle of 20° and the TOI bearing is varied from 22° to 80°. It is seen that power loss is high for very low bearing separation and decreases with an increase in angular separation and is negligible beyond 5° bearing separation. Also, it is observed that, for a given angular separation, the power loss is relatively high for higher SINR, as expected.

Figure 6(c) illustrates the degradation of power loss performance with the spectral coherence between TOI and interference signal for various TOI bearings (50°, 80°, and 110°). The tow-ship is at an angle of 20° with a radiated signal spectral band from 2 kHz to 4 kHz. The SNR of TOI is fixed as -10 dB with radiated signal spectrum (a) 2 kHz to 4 kHz to achieve 100% spectral overlap (b) 1.5 kHz to 3.5 kHz for 75% overlap (c) 1.0 kHz to 3 kHz for 50% overlap (d) 0.5 kHz to 2.5 kHz for 25% overlap. As expected, from Fig. 6(c), it is clear that the power loss is high for 100% spectrum overlap and decreases as spectral overlap decreases.

From Fig. 6, we can deduce that the power loss of the TOI signal is considerable only if the TOI signal has maximum spectrum overlap percentage, very low angular separation with tow ship and high SINR which are of less practical interest. Table 2 illustrates the superior power loss performance of the proposed SIC method with the conventional PCI<sup>19</sup> and ECA<sup>20</sup> method.

**Table 2. Power loss of TOIs corresponding to Fig. 4.**

Method	PCI <sup>19</sup>			ECA <sup>20</sup>			Proposed SIC method		
Bearing (°)	82	106	134	82	106	134	82	106	134
Power loss (dB)	3	2.7	2.3	2	1.3	1	0.36	0.24	0.2

The computational complexity of the proposed method is relatively high compared to the existing methods like IBF, PCI, and ECA. This is mainly due to the handling of higher dimensional space time correlation matrix and its eigenvalue decomposition. Mode decomposition or compressive sensing techniques can be applied to reduce the computational requirements as a future work.

**6. EXPERIMENTAL VALIDATION**

The efficacy of the method is further evaluated for open ocean experimental data. A controlled ocean experiment is conducted in a shallow region of the Arabian Sea, off Kochi, India, wherein the ocean depth was 100 m, approximately. We consider two cases for evaluating the practical performance of the proposed method. In the first case, a simulated shallow ocean target pressure field array data vector is added to the ocean experimental data consisting of ambient ocean noise along with actual towing ship interference. In the second case, the real ocean experimental data consisting of ambient ocean noise, towing ship interference, and two trial ships are used for evaluating the SIC processor.

**6.1 Experimental Details**

To ensure shallow water conditions, initially, the geographical location of the experimental site was identified and characterised by making appropriate measurements on the physical and chemical properties of the medium, ocean bottom characteristics including the sound velocity profile. A towed

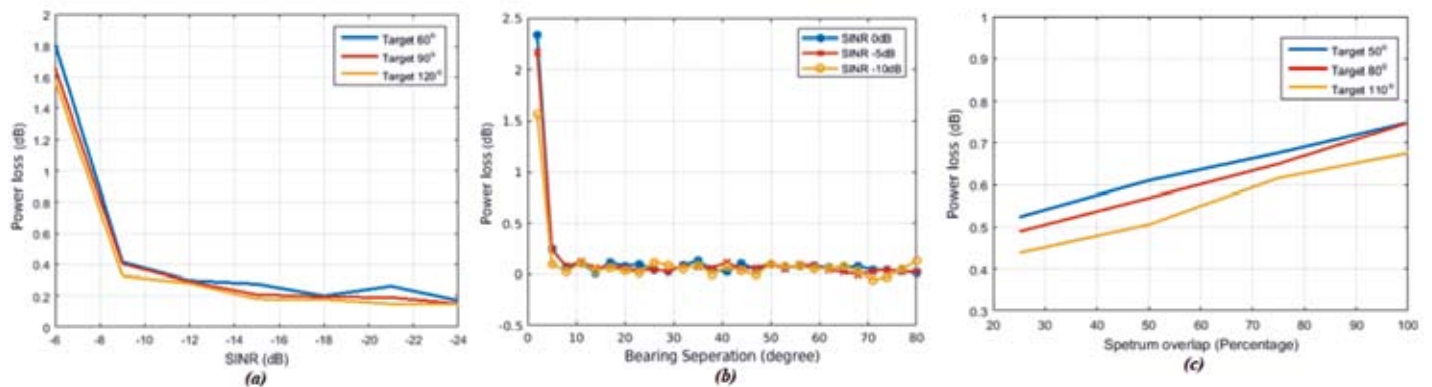


**Figure 6. Power loss in TOI signal. (a) by varying SINR of the targets at different bearing 60°, 90°, 120°. (b) by varying the bearing separation between the TOI and the interference for different SINR values. (c) the spectrum overlap percentage of TOI and interference signal for various TOI bearings 50°, 80°, and 110°.**

array consisting of 96 hydrophones was deployed using an on-board winch from the ORV. The towed array is kept at roughly 20 m depth and 500 m behind the tow ship by adjusting the length of the deployed tow cable and tow ship speed. Two additional ORVs were used for generating the TOI signals for demonstrating the second part of the experiment.

The sensor array supports multi-octave band reception, consisting of 96 non-uniformly spaced sensors to achieve uniform beam width across the bands of operation. There are four octave bands viz. band I up to 500 Hz, band II (500 Hz-1 kHz), band III (1 kHz-2 kHz) and band IV (2 kHz-4 kHz). The 32 hydrophones in the centre part of the array are positioned for band IV with an inter-element spacing of 0.1875 m. Similarly, alternate elements in band IV and 8 elements each on both sides (spaced at 0.375 m) together form 32 elements of Band III and so on.

The acoustic pressure field received by the deployed hydrophone array goes through a chain of analog signal conditioning hardware. The hydrophone output is fed to an ultra-low noise charge amplifier, further passed through a pre-whitening filter and anti-aliasing filter. Using a 24-bit sigma-delta ADC, the data is digitised at Nyquist rate, and then it is packetised into Ethernet frames with proper header structures and payload. The frame ends with a frame check sequence, which is a 32-bit cyclic redundancy check used to detect any in transit corruption of data. This data was stored in a digital data recorder and later archived for analysis.

### 6.2 Case-1: Ocean Experimental Data with Simulated Target

During the ocean experiments, we have recorded the hydrophone array data consisting of tow ship interference in the presence of ambient ocean background. It was ensured that there were no other targets present in the vicinity of the array while recording. Subsequently, the pressure field array data vector corresponding to an acoustic source positioned at an azimuth angle of  $80^\circ$  is synthetically generated and added to the recorded ocean experimental data. This array data vector is processed with and without a SIC processor and the outcome of the response function is shown in Fig. 7. The processing was done in the band IV, 2-4 kHz band. It is observed that, with a SIC processor, the interference of the tow-ship at  $17^\circ$  is significantly reduced with minimum power loss on the target bearing  $80^\circ$ .

### 6.3 Case-2: Experimental Data with Real Targets

In this experiment, the hydrophone array data recording is carried out in the presence of two additional ORVs as target platforms. The ORVs are positioned around  $82^\circ$  and  $143^\circ$  with ranges roughly 5 km and 7 km respectively with respect to the array.

The response function is estimated with and without the SIC processor on the experimental data and is shown in Fig. 8. It is seen that, in the absence of a SIC processor, the own-ship radiation appears prominently at  $15^\circ - 20^\circ$  angular sector and target ORVs around  $82^\circ$  and  $143^\circ$ . The estimated response function with the SIC processor (solid red line) clearly indicates the suppression of tow ship interference

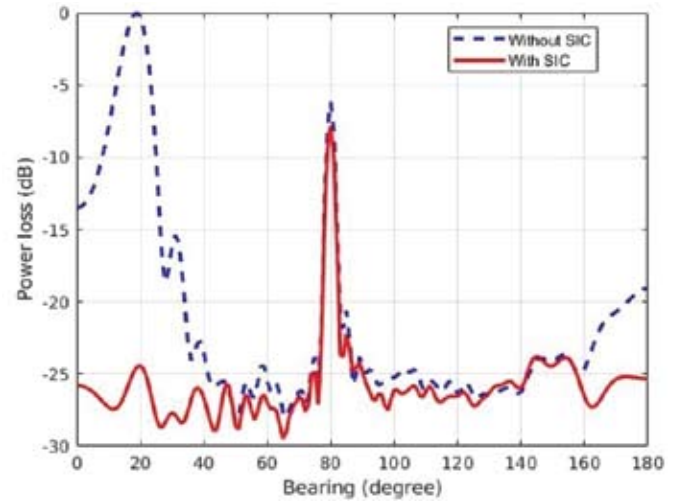


**Figure 7.** Beam power output with and without SIC algorithm on the ocean experimental data added with a simulated target at  $80^\circ$ . Experiment is conducted in the Arabian Sea off Kochi.

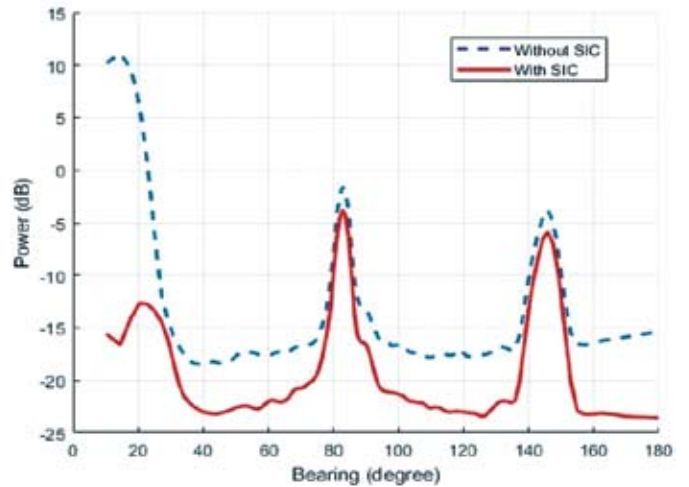


**Figure 8.** Beam power output with experimental data from trials conducted in Arabian sea off Kochi, two ORVs present at around  $82^\circ$  and  $143^\circ$ , and tow ship interference between  $15^\circ - 20^\circ$ .

without affecting the detection performance of TOIs. Also, it is observed that the beam output power in the other steering directions is slightly less compared to the response function without SIC (dotted blue line). The performance may be attributed to the fact that the SIC processor efficiently estimates the spatio-temporal statistics of the tow ship interference and eliminates the multipath arrivals on the sensor array. The SIC processor effectively removes the tow ship feature components in the TOI feature space, which will greatly improve the classification performance of the targets. Table 3 illustrates the superior power loss performance of the proposed method with the conventional PCI<sup>19</sup> and ECA<sup>20</sup> method for the real experimental data.

**Table 3.** Power loss of TOIs corresponding to Fig. 8.

Method	PCI <sup>19</sup>		ECA <sup>20</sup>		Proposed SIC method	
Bearing ( $^\circ$ )	82	143	82	143	82	143
Power loss (dB)	4	3.6	3	2.8	2.1	1.4



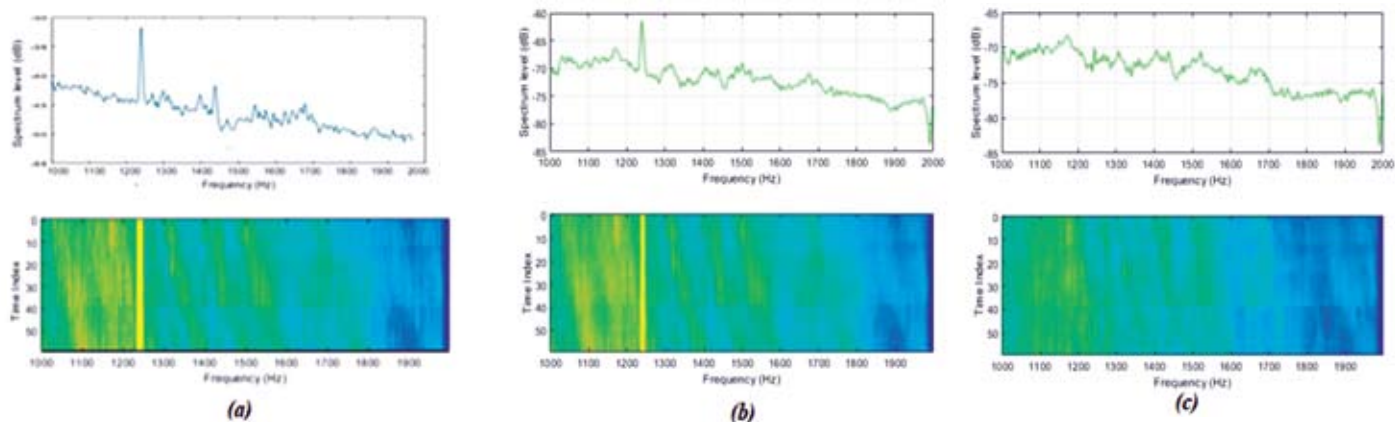


**Figure 9. The amplitude and waterfall graph of the spectrum. (a) beam steered at tow ship direction  $18^\circ$ , (b) beam steered at arbitrary direction  $54^\circ$  without the proposed SIC processor, (c) beam steered at arbitrary direction  $54^\circ$  with the proposed SIC processor. A strong narrowband component 1220 Hz is seen without the pre-processing.**

To demonstrate the capability of the SIC processor to enhance the classification capability, the effect of tow ship interference spectral leakage on any arbitrary steering angle is carried out. Using band III (1 kHz - 2 kHz) sensor data, a beam is steered towards the tow-ship direction to capture and characterise the tow-ship interference.

The beam output is subjected to spectral analysis and the estimated spectrum is shown in Fig. 9(a). It may be noticed that a strong 1220 Hz narrowband component appears in the tow-ship direction which can be considered as a characteristic tonal frequency of the interference and is the most significant source of contamination in the spectrum of other steering directions.

In this context, spectral analysis is carried out on a beam output in an arbitrary steered bearing with and without a SIC processor. Figs. 9(b) and 9(c) shows the beam output power spectrum corresponding to  $54^\circ$  without and with the SIC processor respectively.

In Fig. 9(b), the amplitude and waterfall plot clearly shows the influence of the tow-ship interference in an arbitrary look direction in the absence of the pre-processing. Since the conventional sonar classification techniques rely on the target specific narrow-band components and spectral characteristics, interference spectral leakage significantly degrades the classification performance. Incorporating the SIC processor as a pre-processing technique, the characteristic tonal emanating from the tow-ship is significantly suppressed, and it is evident in both the amplitude and waterfall graph presented in Fig. 9(c).

It is demonstrated that the proposed SIC method is a suitable pre-processing algorithm for shallow water towed array sonar operations, where the tow ship interference is a significant contributor to the degradation of the detection, localisation and classification performance.

## 7. CONCLUSION

A new perception of interference cancellation is introduced in this paper with a prime objective to detect and classify stealthy long-range targets in the presence of strong interference generated by own ship and ambient noise in a shallow ocean scenario. In this paper, we have developed a

spatio-temporal processing technique combined with subspace analysis, customised to cancel the self-interference by exploiting the space-time covariance characteristics of the tow ship radiations.

The method is initially verified by modelling the tow ship interference, signal radiated from the targets and the ambient noise in a shallow ocean environment. The interference suppression in the beam response function, power loss associated with TOI and the spectral leakage of the own ship's characteristic narrow-band components into the spectrum of any arbitrary steering direction were investigated, demonstrating the efficacy of the proposed SIC processor as compared with ECA and PCI methods. It is observed to be robust against array imperfections as well. The proposed method significantly reduces the effect of own ship noise on the spatial response function as well as in the spectral domain. This brings in good improvement in the quality of the target detection and classification, which are critical functions of a passive sonar in the event of a warfare or conflict.

The robustness of the proposed algorithm is validated by the open ocean experiment involving three ocean research ships in the coastal region of the Arabian Sea at Off-Kochi area of India. The close agreement between the results from simulations and the ocean experiment suggest that this method is quite useful in maritime operations. The proposed method may be extended to monitor other platforms like unmanned automatic vessels and subsurface targets. Investigation in this important oceanic research field is in progress with the authors and the result would be communicated in future.

## REFERENCES

1. Urick, R. J. Principles of Underwater Sound. McGraw Hill, Inc., (3rd ed.), 1983.
2. Lemon, S. J. Towed-array history, 1917-2003, *IEEE J. Ocean. Eng.*, 2004, **29**(2), 365–373. doi: 10.1109/JOE.2004.82979
3. Hinich, M. J.; Marandino, D. & Sullivan, E. J. Bispectrum of ship-radiated noise. *J. Acoust. Soc. Amer.*, 1989, **85**(4), 1512–1517. doi: 10.1121/1.397352

4. Brekhovskikh, L. M. & Lysanov, Yu. P. Fundamentals of Ocean Acoustics. AIP Press, New York, (3rd ed.), 2003.
5. Kuperman, W. A. & Lynch, J. F. Shallow-water acoustics. *Physics Today*, 2004, **57**(10), 55–61.  
doi: 10.1063/1.1825269
6. Vaccaro, R. J. The past, present and future of under-water acoustic signal processing. *IEEE Signal Process. Mag.*, 1998, **15**(4), 21–51.  
doi: 10.1109/79.689583.
7. Jian, Li. Robust Adaptive Beamforming. Wiley series in Telecommunications, 2006.
8. Robert, M. K. & Beerens, S. P. Adaptive Beamforming Algorithms for Tow Ship Noise Cancelling. *In Proc. UDT Europe*, 2002.
9. Vaccaro, R. J.; Chhetri, A. & Harrison, B. F. Matrix filter design for passive SONAR interference suppression. *J. Acoust. Soc. Amer.*, 2004, **115**(6), 3010–3020.  
doi:10.1121/1.1736653.
10. Bin, Zhang. Research on Directional Interference Canceling. *In Proc. Intelligent Information Technology and Security Informatics*, IEEE Symposium, 2010, 549–552.  
doi: 10.1109/IITSI.2010.96
11. Li, Y.; Sun, C.; Yu, H. & Wang, L. A Technique of Suppressing Towed Ship Noise. *In IEEE International Conference on Signal Processing, Communications and Computing*, 2011, 1–4.  
doi: 10.1109/ICSPCC.2011.6061631
12. Jia, Feng; Nan, Zou; Yan, Wang & Yu, Hao. Methods of suppressing tow ship noise with a horizontal linear array. *J. Acoust. Soc. Amer.*, 2018, **143**(3), 3010–3020.  
doi: 10.1121/1.5036438.
13. Cheng, C.; & Venugopalan, Pallayil. Noise cancellation for an autonomous underwater vehicle-towed thin line array through recursive adaptive filtering. *J. Acoust. Soc. Amer.*, 2017, **141**.  
doi: 10.1121/1.4988873
14. Cheng, C.; Venugopalan, Pallayil, Mandar, Chitre. Design of an adaptive noise canceller for improving performance of an autonomous underwater vehicle-towed linear array. *Ocean Engineering*, 2020, **202**.  
doi: 10/1016/j.oceaneng.2019.106886
15. Sullivan, E. J. & Candy, J. V. Enhanced Processing for a Towed Array Using an Optimal Noise Canceling Approach. *In Proc. IEEE Oceans Conf.*, 2005, **2**, 1093–1098.
16. Lee, H.; Ahn, J.; Kim, Y. & Chung, J. Direction-of-arrival estimation of far-field sources under near-field interferences in passive sonar array. *IEEE Access*, 2021, **9**, 28413–28420.  
doi: 10.1109/ACCESS.2021.3059157
17. Qiu, L.; Lan, T. & Wang, Y. A sparse perspective for direction-of-arrival estimation under strong near-field interference environment. *Sensors*, 2019, **20**(1), 1–21.  
doi: 10.3390/s20010163
18. Juan; H.; Song, M. & JiangQiao, Li. Research on suppression for tow ship interference. *J. Acoust. Soc. Amer.*, 2018, **144**(3), 3010–3020.  
doi: 10.1121/1.5068506
19. Kirsteins; Tufts, D. Adaptive detection using low rank approximation to a data matrix. *IEEE Trans. Aerosp. Electron. Syst.*, 1994, **30**, 55–67.  
doi: 10.1109/7.250406
20. Harrison, B. F. The Eigen component association method for adaptive interference suppression. *J. Acoust. Soc. Amer.*, 2004, **115**(5), 2122–2128.
21. Chen, W.; Zhang, W.; Wu, Y.; Chen, T. & Hu, Z. Joint algorithm based on interference suppression and Kalman filter for bearing-only weak target robust tracking. *IEEE Access.*, 2019, **7**, 131653–131662.  
doi: 10.1109/ACCESS.2019.2940956
22. Chen, W.; Zhang, W.; Wu, Y.; Chen, T. & Hu, Z. Review of Interference Suppression Algorithms for Passive Sonar. *In 2<sup>nd</sup> IEEE International Conference on Information Communication and Signal Processing*. 2019, 256–261.
23. Pekeris, C. L. Theory of propagation of sound in a half-space of variable sound velocity under conditions of formation of a shadow zone. *J. Acoust. Soc. Amer.*, 1946, **18**(2), 295–315.  
doi: 10.1121/1.1916366
24. Jensen, F. B.; Kuperman, W. A.; Porter, M. B. & Schmidt, H. Computational Ocean Acoustics. Springer Science amp, Business Media. 2011.
25. Porter, M.; & Reiss, E. L. A numerical method for ocean-acoustic normal modes, *J. Acoust. Soc. Amer.*, 1984, **76**(1), 244–252.  
doi: 10.1121/1.391101
26. Guerci, J. R.; Goldstein, J. S. & Reed, I. S. Optimal and adaptive reduced-rank STAP. *IEEE Trans. Aerosp. Electron. Syst.*, 2000, **36**(2), 647–663.  
doi: 10.1109/7.84525
27. Mio, K.; Chocheyras, Y.; & Doisy, Y. Space time adaptive Processing for low frequency sonar. *In Proc. IEEE Oceans Conf.*, 2000, **36**(2), 1315–1319.
28. Brennan, L. E. & Reed, L.S. Theory of adaptive radar. *IEEE Trans. Aerosp. Electron. Syst.*, 1973, **9**(2), 237–252.  
doi: 10.1109/TAES.1973.309792
29. Klemm, R. Space Time Adaptive Processing: Principles and Applications. London IEE press, 2002.
30. Wu, J.; Cao, X.; Chen, Y. & Sun, J. Tow Ship Interference Suppression for Towed Array Sonar via Subspace Reconstruction. *In Proc. of IEEE 10th International Conference on Wireless Communications and Signal Processing*, 2018, 1–7.  
doi: 10.1109/WCSP.2018.8555587
31. Haimovich, A. M. & Bar-Ness, Y. An Eigen analysis interference canceller. *IEEE Trans. Signal Processing*, 1991, **39**(1), 76–84.  
doi: 101109/78.80767
32. Ren, S.; Ge, F.; Guo, X. & Guo, L. Eigenanalysis-based adaptive interference suppression and its application in acoustic source range estimation. *IEEE J. Ocean. Eng.*, 2015, **40**(4), 903–916.  
doi: 10.1109/JOE.2014.2359378
33. Kumar, N. S.; Philip, D.J. & Anand, G. V. Source number estimation in shallow ocean by gerschgorin disks using

- acoustic vector sensor array. *J. Network Innovative Comput.*, 2013, **1**, 109-118.
34. Kumar, N. S.; Anand, G. V.; Roul, S. & Philip, D. J. Source Number Estimation in Shallow Ocean by Acoustic using Vector Sensor Array using Gerschgorin Disks. *In Proc. of IEEE 12th International Conference on Intelligent Systems Design and Applications*, 2012, 83-88. doi: 10.1109/ISDA.2012.6416517
  35. Van Trees; Harry, L. Optimum Array Processing - Part IV of Detection, Estimation, and Modulation Theory. John Wiley Sons. Inc. Publications, 2002. pp. 19-42.
  36. Porter, M. B. The KRAKEN normal mode program. SACLANT Undersea Research Centre, La Spezia, Italy, Report No. SM-245, 1991.
  37. Buckingham, M. J. A Theoretical model of ambient noise in a low-loss shallow water channel. *J. Acoust. Soc. Amer.*, 1980, **67**(4), 1186-1192. doi: 10.1121/1.38416

#### ACKNOWLEDGEMENT

The authors thank Shri S. Vijayan Pillai, Director, Naval Physical and Oceanographic Laboratory, DRDO, Ministry of Defence for the support and permission to publish the paper in the Defence Science Journal.

#### CONTRIBUTORS

**Ms Remadevi M.** received ME in Telecommunications from Indian Institute of Science, Bangalore in 2004 and presently pursuing PhD from CUSAT, Kochi. She is a senior scientist with the Naval Physical and Oceanographic Laboratory (NPOL), Kochi, India. She has made significant contributions to the design and development of sonar systems. Her research interests

include sonar signal processing, compressed sensing and underwater communications.

Her contribution towards this research is the design and implementation of the algorithm, data collection and analysis as well as primary manuscript preparation.

**Dr N. Sureshkumar** received his PhD in 2014 from Defence Institute of Advanced Technology, Pune, India. He is a senior scientist with NPOL, Kochi. His research interests include underwater acoustics, sonar signal processing, sparse array processing, vector sensors etc.

His contribution towards this research is the identification of multiple objectives of the work and evaluation of the results. Also, he contributed by providing overall guidance to the development of the designed algorithm and manuscript corrections.

**Dr R. Rajesh** received PhD in physics from Jamia Millia Islamia, New Delhi, in 2005. In 2000, he joined the Laser Science and Technology Center, New Delhi, and worked on high-power lasers. Since 2008, he has been with NPOL, Kochi, and focuses on fiber optic underwater acoustic sensors for sonar applications.

He acted as an advisor to the research work reported in the paper. He contributed by rendering overall guidance and provided vital ideas and key suggestions in this research.

**Dr T. Santhanakrishnan** received PhD from Anna University, Chennai, India, in 1998. He joined as a Scientist of DRDO in India at NPOL, Kochi, where he initiated the basic and applied research in opto-electronics systems for maritime applications. His current interests include fiber optic hydrophones, PZT thin film based acoustic sensors and sonar signal processing. He has helped in the experimental part of the research and has also revised the draft of the manuscript to make it final.